Short-Lived Radical Intermediates in the Photochemistry of Glucose Oxidase

Lipsa Nag, Andras Lukacs, Marten H. Vos

COMMUNICATION

Short-lived radical intermediates in the photochemistry of glucose oxidase

Lipsa Nag[a], Andras Lukacs[b] and Marten H. Vos*[a]

Abstract: Glucose oxidase is a flavoprotein that is relatively well-studied as a physico-chemical model system. The flavin cofactor is surrounded by several aromatic acid residues that can act as direct and indirect electron donors to photoexcited flavin. Yet, the identity of the photochemical product states is not well established. We present a detailed full spectral reinvestigation of this issue using femtosecond fluorescence and absorption spectroscopy. Based on a recent characterization of the unstable tyrosine cation radical $TyrOH^{\bullet+}$, we now propose that the primary photoproduct involves this species, which was previously not considered. Formation of this product is followed by competing charge recombination and radical pair stabilization reactions that involve proton transfer and radical transfer to tryptophan. A minimal kinetic model is proposed, including a fraction of $TyrOH^{\bullet+}$ that is stabilized up to the tens of picoseconds timescale, suggesting a potential role of this species as intermediate in biochemical electron transfer reactions.

Nature employs charge transfer reactions to perform a large variety of fundamental biochemical processes in proteins. Such reactions almost invariably involve specialized cofactor molecules. Among them, flavins are abundantly found; they are highly versatile as they can exist in multiple physiologically relevant oxidation states - oxidized, one-electron reduced and two-electron reduced- and protonation states[1]. On the other hand, radical forms of tyrosine (TyrOH) and tryptophan (TrpH) amino acids, that are constituents of the protein backbone, are also frequently involved as intermediates in such reactions. While in the neutral ground states both these amino acid residues absorb only in the UV region, their radical states (both protonated cation and deprotonated neutral) have distinct absorption bands in the visible region[2, 3]. In flavoproteins, photoreduction of excited flavin by electron transfer from nearby TyrOH or TrpH residues is an efficient fluorescence quenching mechanism. The role of such reactions has been investigated in naturally light-active sensor and photoenzyme flavoproteins, notably that of DNA photolyase[4-7], cryptochrome[8] and BLUF domain blue light sensing proteins[9-11]. However, they also occur in many non-photoactive flavoproteins, where they can be used as a conformational probe[12, 13]. Due to the flavin extinction coefficients being of similar amplitude, flavoproteins also provide a suitable environment to detect and characterize intermediates of TyrOH and TrpH by optical spectroscopy. The radical intermediates involving TyrOH and TrpH (both protonated and neutral) have been characterized spectroscopically in protein systems[2-4, 14]. In particular, recently the highly unstable $TyrOH^{\bullet+}$ radical (pK ~-2) was spectrally characterized for the first time by our group as a short-lived (~3 ps) intermediate in C51A modified (avoiding flavin adduct formation) TrmFO (itself a non-light-activated enzyme), where tyrosine and the flavin isoalloxazine ring are very close[14]. $TyrOH^{\bullet+}$ had been invoked as a functional intermediate in other protein systems[15, 16], though too short-lived to be detectable. Given the potential relevance of this state, we have engaged to investigate whether it may occur more generally in tyrosine-flavin systems. One such potential candidate is glucose oxidase from *Aspergilus niger*.

Glucose oxidase (GOX) is a widely used flavo-enzyme in the food[17, 18] and pharmaceutical industries[19]. It is also used in biofuel cells[20] and is a major component of glucose biosensors[21]. GOX is homodimeric, with an FAD molecule bound non-covalently at the active site of each subunit. In GOX from *Aspergilus niger*, there are five redox-active residues in the vicinity of the FAD isoalloxazine (Fig. 1): Tyr515 (at 4.0 Å ring-ring distance in the crystal structure), Tyr68 (4.3 Å), Trp111 (7.0 Å), Tyr565 (8.3 Å) and Trp426 (8.4 Å). Even though it does not rely on photoactivation for its function, the photochemistry of GOX has been studied relatively extensively using ultrafast spectroscopic techniques.

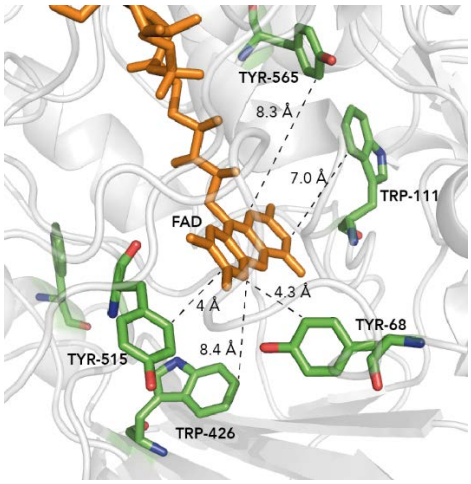

Figure 1. Potential redox-active residues near the active site of glucose oxidase from *Aspergilus niger* (PDB: 1CF3[22]). Distances between the isoalloxazine ring of the FAD and the tyrosine and tryptophan aromatic rings are shown.

Early time-resolved fluorescence studies performed by Mataga *et al*. indicated that the fluorescence decay, occurring predominantly on the few-picosecond timescale, was multiphasic. The first electron transfer step was proposed to be barrierless, involving the closest-lying residues Tyr515 and Tyr68 as potential

[a] Dr. L. Nag, Dr. M.H. Vos
LOB, CNRS, INSERM
Ecole Polytechnique, IP Paris
91128 Palaiseau, France
E-mail: marten.vos@polytechnique.edu
[b] Dr. A. Lukacs
Department of Biophysics, Medical School
University of Pecs
Hungary

Supporting information for this article is given via a link at the end of the document.

electron donors to the FAD[23, 24]. Zhong and Zewail performed transient fluorescence and absorption spectroscopy at selected wavelengths, and proposed that electron transfer could occur from both TyrOH and TrpH since none of the surrounding redox-active residues stack completely with the FAD[25]. They assigned transient absorption phases on the 30-ps and nanosecond timescale to charge recombination. Fujiwara and Mizutani studied photoinduced electron transfer in GOX using transient UV resonance Raman spectroscopy[26]. Based on the intermediate loss in intensity of Trp-assignable bands (that are stronger than Tyr-assignable UVRR features) they proposed the involvement of Trp rather than Tyr as electron donor to FAD. However, they did not explicitly rule out the possibility of the involvement of the two close-lying Tyr residues in electron transfer.

More recently, Lukacs *et al.* performed the first study on GOX using time-resolved IR and visible absorption spectroscopy with full spectral resolution[27]. Here, IR features associated with the rise in a few picoseconds and decay on the tens of picoseconds timescale were also tentatively ascribed to tryptophan radical intermediates. However, the spectrum in the visible associated with charge recombination was rather poorly reproduced with model spectra of radical intermediates available at the time. They show some reminiscence, by contrast, with the spectrum recently assigned to the $FAD^{\bullet-}TyrOH^{\bullet+}$ radical pair[14].

The latter observation motivated us to reinvestigate the complex photochemistry of GOX using spectrally-resolved ultrafast fluorescence and absorption spectroscopy. Based on spectral modeling we propose a series of photoproducts formed during charge transfer in photoactivated GOX that in particular include the $TyrOH^{\bullet+}$ species, and a minimal kinetic scheme is put forward.

Fig. 2 (left) shows the timetrace for the fluorescence decay at 530 nm, near the fluorescence maximum (Fig. 2, right). The signal strongly decays on the timescale of a few picoseconds. A small fraction of long-lived fluorescence remains after 10 ps, indicating the presence of a small amount of free FAD.

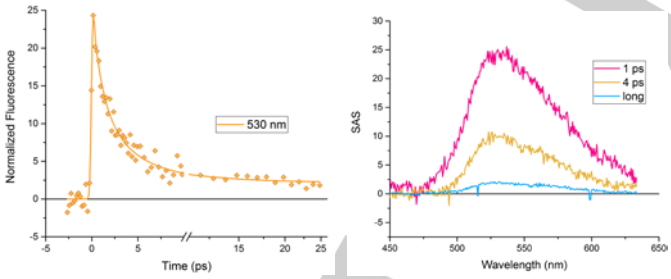

Figure 2. (left) Timetrace at 530 nm for the transient fluorescence spectra on a lin-log scale. Scale is linear till 10 ps and logarithmic thereafter. (right) Absolute species associated spectra (SAS) with time constants.

The global analysis indicates that, as reported by previous workers[23-25], the decay is modestly non-exponential in GOX. The time-constants obtained from the fit were 1 ps (~70%), 4 ps, with similar associated spectra (Fig. 2, right) and a minor long phase (longer than the timescale of the experiment). This modestly non-exponential behavior presumably reflects some conformational heterogeneity, as often observed in protein systems.

To visualize any product states formed, transient absorption experiments were performed. The kinetics (Fig 3, left) are clearly wavelength-dependent. The timetrace at 573 nm, where the negative signal reflects stimulated emission, evolves similar to that of the fluorescence (Fig. 2, left). At different wavelengths slower phases are clearly present, including those with opposing sign (490 nm), as also reported by others[25, 27].

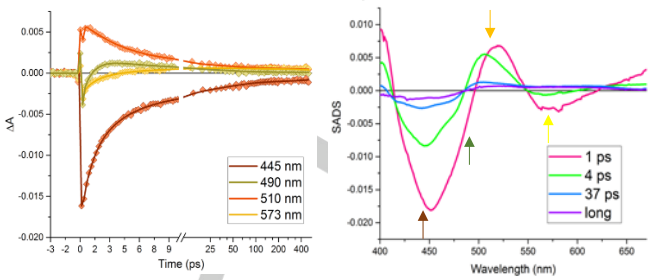

Figure 3. (left) Transient absorption kinetics. Scale is linear untill 10 ps and logarithmic thereafter. (right) Species associated difference spectra (SADS) associated with time constants 1 ps, 4 ps, 37 ps and a long-lived phase. The arrows correspond to the kinetics in the left panel.

In the global analysis of the transient absorption data, a minimum of four phases were required, of which two had a time constant below 10 ps. Using 1-ps and 4-ps time constants retrieved from the fluorescence analysis, a satisfactory fit was obtained with an additional 37-ps phase and a long-lived phase; the corresponding species associated difference spectra (SADS) are shown in Fig. 3 (right). The 1-ps phase is dominant and has a characteristic excited state spectrum, in agreement with the fluorescence results. The 4-ps SADS is reminiscent of the 1-ps phase, consistent with excited-state contributions. Notably, the ratios of the 4-ps phase and 1-ps phases are comparable for both fluorescence and the negative transient absorption features around 570 nm reflecting stimulated emission. However, the relative amplitude and shape of the induced absorption band near 500 nm are markedly different. This indicates that the spectral evolution on the 4-ps timescale does not solely reflect excited state decay.

In the following, we will further analyze the spectral evolution through modeling of the SADS. Here, the FAD_{ox} ground state spectrum of the GOX sample is used, as well as the spectra for $FAD^{\bullet-}$ and $FADH^{\bullet}$ in GOX as described in the literature[28, 29]. Furthermore, published spectra for $TyrO^{\bullet}$ and $TrpH^{\bullet+}$[2, 3, 30] are used.

The initial state ($SADS_{1ps}$) is assigned to the excited state FAD*, and contains contributions from ground state bleaching, stimulated emission and excited state absorption. As mentioned above, $SADS_{4ps}$ reflects FAD* and contains a contribution from a different state. The spectrum of this state is denoted with $S(\lambda)$ and it apparently also decays with a time constant of ~4 ps. As no ground state absorption occurs in this spectral region, the negative absorption around 570 nm can only be due to stimulated emission. Hence $S(\lambda)$ was determined by subtraction of a fraction y (determined at 0.4 from the analysis of the fluorescence decay) of $SADS_{1ps}$ from $SADS_{4ps}$ so that the stimulated emission feature vanished:

$$S(\lambda) = SADS_{4ps} - y \times SADS_{1ps} \quad (1)$$

The resulting spectrum $S(\lambda)$ (Fig. 4, green) is qualitatively similar to the spectrum we previously assigned to the difference of the

$FAD^{\bullet-}$–$TyrOH^{\bullet+}$ and FAD_{ox} states [14]. Therefore we modeled S(λ) as a combination of flavin spectra and a contribution $X_{4ps}(\lambda)$ as

$$S(\lambda) = \alpha[FAD^{\bullet-} - FAD_{ox}] + X_{4ps}(\lambda) \quad (2)$$

Here, the scaling factor *α* was taken such that the scaled $FAD^{\bullet-}$ *minus* FAD_{ox} extinction spectrum (blue, Fig. 4) matches the bleaching in *S(λ)* (green, Fig. 4) in the blue part of the spectrum (<440 nm). Indeed, the obtained $X_{4ps}(\lambda)$ spectrum has an absorption peak at ~490 nm, as the spectrum assigned to $TyrOH^{\bullet+}$ in a TrmFO variant[14]. We note there are also significant spectral differences, as will be discussed below, and the need of the subtraction procedures of Eqn. 1 and 2 yields some uncertainty in the precise shape of the band, but significant absorption in this spectral region is always required. We therefore suggest that $TyrOH^{\bullet+}$ is also formed in GOX.,

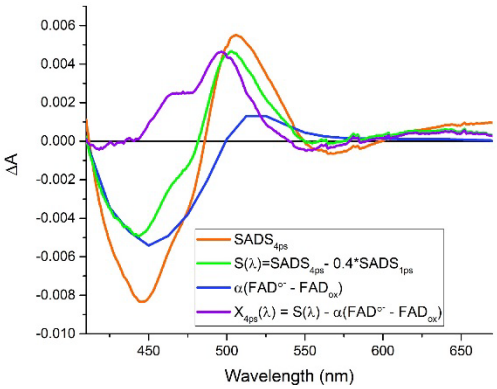

Figure 4. Spectral analysis of the 4-ps phase SADS. The excited state contribution (from the 1-ps phase) has been subtracted from $SADS_{4ps}$ to obtain *S(λ)*. *S(λ)* is described in terms of the ($FAD^{\bullet-}$–FAD_{ox}) spectrum and a contribution $X_{4ps}(\lambda)$ as described in the text.

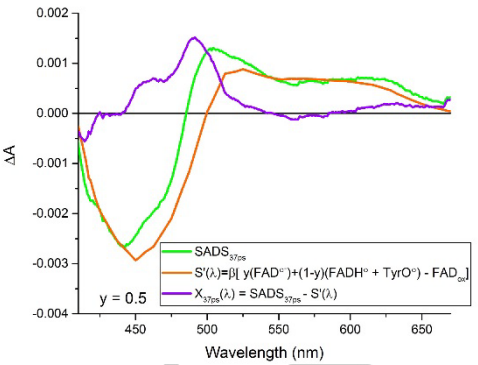

Figure 5. Spectral deconvolution of the 37-ps phase SADS. The model spectrum *S'(λ)* is constructed using a combination of known $FAD^{\bullet-}$, $FADH^{\bullet}$ and $TyrO^{\bullet}$ model spectra. $X_{37ps}(\lambda)$ is the spectral contribution remaining after modelling *S'(λ)* with *y*=0.5.

The analysis of the 37-ps phase SADS (Fig. 5) appears more complex. The small peak around 500 nm suggests a remaining contribution of $TyrOH^{\bullet+}$. In addition, the broad absorption in the 550-650 nm range is indicative of a contribution of $FADH^{\bullet}$. This could be due to partial proton transfer from $TyrOH^{\bullet+}$ to $FAD^{\bullet-}$. Therefore, this SADS was modelled as

$$S'(\lambda) = \beta\,[y \times (FAD^{\bullet-}) + (1-y)(FADH^{\bullet} + TyrO^{\bullet}) - FAD_{ox}] \quad (3)$$

$$X_{37ps}(\lambda) = SADS_{37ps} - S'(\lambda) \quad (4)$$

Here, the scaling factor *β* was taken such that *S'(λ)* matches $SADS_{37ps}$ in the bleaching blue part of the spectrum (<440 nm). The factor *y* (reflecting the fraction of proton transfer) was taken to be at 0.5, which corresponds to an optimum overlap in the 550-650 nm range where only the $FADH^{\bullet}$ contribution is significant. $X_{37ps}(\lambda)$ corresponds to the spectral contribution that remained after taking contributions from the model spectra into account.

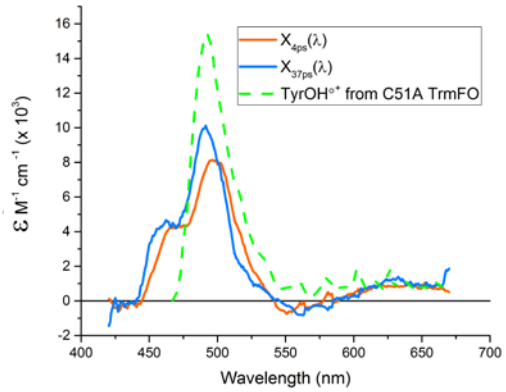

Figure 6. Comparison of $TyrOH^{\bullet+}$ spectra obtained from GOX SADS deconvolution with that from C51A TrmFO.

Fig. 6 shows that the $TyrOH^{\bullet+}$ spectrum derived from the modelling of the 37-ps phase, $X_{37ps}(\lambda)$, is very similar to that derived from the modelling of the 4-ps phase, $X_{4ps}(\lambda)$, implying consistency of the approach. These spectra compare reasonably well with that proposed for $TyrOH^{\bullet+}$ from TrmFO C51A[14] with the characteristic strong peak at ~490 nm and no significant spectral features on the red side. This strongly suggests that $TyrOH^{\bullet+}$ is formed as an intermediate in GOX and is stabilized for a longer timescale than C51A TrmFO as it decays in tens of ps. It appears that in the GOX spectra, a fraction of the oscillator strength of the 490 nm band of the TrmFO spectrum is blue-shifted to ~460 nm. This may be due to the different protein environment. It cannot be excluded that the details of the assumptions underlying the modelling also contribute to this difference.

Finally, we address the SADS associated with the long-lived phase (Fig. 7). Comparing with the 37 ps SADS, here the peak at ~500 nm is decreased with respect to the $FADH^{\bullet}$ feature. Hence, modelling with the same components as with the 37-ps phase did not yield satisfactory results. However, assuming that a fraction of the cation radical is located on a tryptophan residue rather than tyrosine allows satisfactorily modelling the SADS as

$$SADS_{long} = [y\{FAD^{\bullet-} + z(TyrOH^{\bullet+}) + (1-z)TrpH^{\bullet+}\} + (1-y)(FADH^{\bullet}TyrO^{\bullet}] - FAD_{ox} \quad (5)$$

Here, the $TyrOH^{\bullet+}$ spectrum used is the one which was calculated for the 37-ps phase (Fig. 5). The factor *y* (0.4), reflecting the total fraction of charged radical states, was determined from the ratio of the $FADH^{\bullet}$ induced absorption feature >620 nm (where $TrpH^{\bullet+}$ does not absorb) and the FAD_{ox} bleaching, and *z* (0.5), reflecting

the fraction of charged radical states where the charge remains on a tyrosine, from adjusting the remainder of the spectrum. The modest deviations from the SADS spectrum in the 430-500 nm region may be due to changes in the $TyrOH^{\bullet+}$ spectrum.

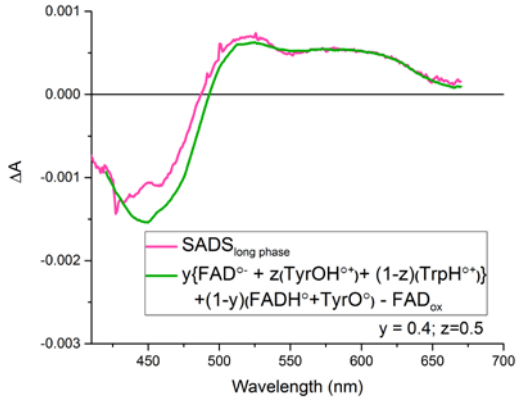

Figure 7. Spectral deconvolution of the long phase SADS. The model (in green) is constructed using a combination of model spectra of $FAD^{\bullet-}$, $TyrOH^{\bullet+}$, X_{37ps}, Fig. 6), $FADH^{\bullet}$, $TyrO^{\bullet}$,and $TrpH^{\bullet+}$.

Altogether, in GOX the spectral evolution upon impulsive photoexcitation is complex, with multiphasic FAD* decay (dominated by ~1 ps and ~4 ps phases) partly taking place on similar time scales as product state evolution. The product state evolution can be described with phases with time constants of 4 ps and 37 ps and with a longer-lived phase. The time scales of the excited and product state decay are generally consistent with those reported in previous time-resolved studies[23-27]. The 4-ps phase was modelled using FAD_{ox} and $FAD^{\bullet-}$ spectra (after removal of the excited state contribution). The 37-ps phase was modelled using FAD_{ox}, $FAD^{\bullet-}$, $FADH^{\bullet}$ and $TyrO^{\bullet}$ model spectra. Yet, for the 4-ps and 37-ps phases an additional contribution with a spectral component strongly resembling that of the $TyrOH^{\bullet+}$ spectra obtained in TrmFO[14] was required, with a characteristic peak near 490 nm.

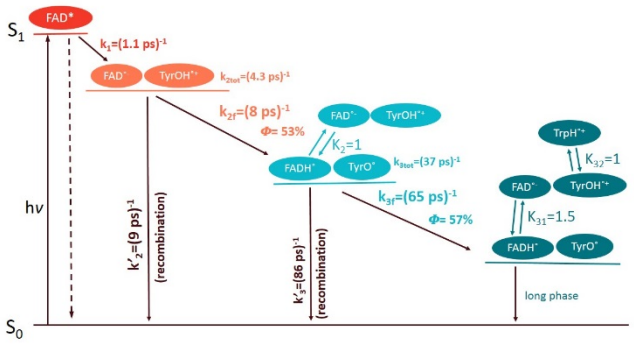

Figure 8. Minimal kinetic model describing the electron transfer reactions. k_i are forward reaction rates and k_i' are recombination rates. The yield for each step is indicated by ϕ. K_i represent pseudo-equilibrium constants.

A comprehensive minimal model of the involvement of Tyr and Trp radicals in light-induced charge separation and subsequent charge recombination processes in GOX can be elaborated, taking into account all spectral features and incorporating both electron and proton transfer (Fig 8). The determination of the values for the parameters in this scheme is detailed in the Supporting Information. For simplicity, this scheme ignores the heterogeneity in the FAD* decay and focusses on its ~1 ps component. According to this model, the product state $FAD^{\bullet-}TyrOH^{\bullet+}$ is formed in 1.1 ps. Following this, it decays with an efficiency of ~50% to a mixture of states of $FAD^{\bullet-}TyrOH^{\bullet+}$ and $FADH^{\bullet}TyrO^{\bullet}$ with a pseudo-equilibrium constant K_2~1. Charge recombination, with a similar intrinsic rate of ~$(8ps)^{-1}$, competes with the formation of this mixture of states. After this stage, the system evolves into a different mixture of states with a ~57% yield, again in competition with charge recombination, with an intrinsic rate of ~$(90\ ps)^{-1}$. This mixture contains the same states as the preceding mixture, but with a pseudo-equilibrium constant K_{31}=1.5. In addition, the $TyrOH^{\bullet+}$ is itself in equilibrium with $TrpH^{\bullet+}$ with a pseudo-equilibrium constant K_{32}=1. The products remaining after the second forward reaction are a mixture of radicals which decay on a longer timescale than the experiment. The decay of $TyrOH^{\bullet+}$ (by charge recombination, proton transfer to the reduced flavin or electron transfer from a tryptophan) on the picosecond timescale is in general agreement with its presumed unstable character ((pK ~-2). The finding that this decay is only gradual and incomplete may reflect protein relaxation reactions required for further charge transfer steps.

This scheme is reminiscent of the charge stabilization schemes elaborated for photolyase and cryptochrome photoactivation[5, 6, 31, 32] where hopping of the positive charge between different residues occurs in competition with charge recombination and sometimes proton transfer. As the FAD in GOX is surrounded by several Tyr residues (Tyr68, Tyr515 and Tyr565, neither in hydrogen-bonding interaction with the flavin ring) which could each be involved in the charge transfer pathway (Fig. 1), a similar mechanism involving different residues is possible here. For instance, the initial step likely involves the closest-lying Tyr515 and/or Tyr68, and further steps may involve Tyr565 and Trp426. The latter states that appear to be mixtures of different radical pairs can be considered as in pseudo-equilibrium: the equilibration between these radical pairs occurs faster than their formation time. More subtle equilibrations involving protein relaxations are, in principle, also possible. To identify the role of each residue as an electron transfer candidate more precisely, experiments will have to be performed on mutants of GOX where each such residue would be substituted with a redox-inactive residue such as phenylalanine. Our conclusion that with the observed proximity of tyrosine residues to the flavin in the crystal structure (Fig. 1), and with earlier suggestions based thereon in ultrafast fluorescence and absorption studies[23-25]. Based on changes in tryptophan-assignable bands in picosecond transient UV Raman spectroscopy, however, rather the involvement of the more remote tryptophan residues in the photochemistry of GOX[26] was proposed. The weaker absorption of tyrosine in the UV may have influenced this interpretation.

In conclusion, we have identified photoproducts formed during charge transfer in photo-excited GOX from *Aspergilus niger*. In particular, the intermediate $TyrOH^{\bullet+}$, which has been identified in C51A TrmFO, is also proposed as a photoproduct in GOX. Based on these results, we also propose a minimal kinetic scheme for charge transfer in GOX.

An important conclusion from this work is that a spectrum characteristic of $TyrOH^{\bullet+}$ is required to comprehensively describe the spectral evolution of GOX using femtosecond absorption spectroscopy. This spectrum (Fig. 6) has a characteristic band at ~490 nm, as well as a minor feature on the blue side (~450-475 nm), different from the one observed in TrmFO C51A, that may be characteristic for the GOX environment. Additionally, this study suggests that the transient population of $TyrOH^{\bullet+}$ can be stabilized up to a timescale of tens of picoseconds. This timescale is beyond the typical timescale of vibrational cooling in proteins. This lends further support to the idea that the spectral feature reflects a true intermediate, and not a spectral relaxation of the flavin as recently suggested[33].

The role of individual residues in the charge transfer processes in GOX could not be inferred from the complex data and will require additional experiments associating site-directed mutagenesis and spectroscopy.

Experimental Section

GOX from *Aspergillus niger* was purchased from Sigma and dissolved into a 60 mM sodium phosphate buffer at pH 8.0. Both transient fluorescence and transient absorption experiments were performed in 1 mm-optical pathlength cells. The optical density of the sample was adjusted to ~0.3 at the absorption maximum near 450 nm.

The time-resolved fluorescence setup uses a Kerr gate and has been described before[14, 34]. The excitation pulse centered at 390 nm is obtained by frequency-doubling, using a BBO crystal, part of the 780-nm pulse from the Ti:sapphire laser/amplifier system (Quantronix Integra-C) operating at 1 kHz. The remaining 780-nm beam is led through a motorized delay-line and focused into the Kerr medium where it spatially overlapped the fluorescence from the sample. Data were collected up to a delay of 10 ps with Suprasil as a Kerr medium (response time ~200 fs) and to 25 ps with CS_2 (response time ~1 ps). Data in the 5-10 ps range in both experiments were used to overlay the data and construct the shown kinetics.

Multicolor time-resolved absorption spectra were performed on an instrument operating at 500 Hz as described[14] with pump pulses centered at 390 nm and continuum broadband probe pulses. The pump beam was polarized at magic angle with respect to the probe beam to avoid photoselection effects. The excitation energy for all measurements was kept at 150 nJ per pulse to avoid non-linear signals. Transient absorption data were collected upto 500 ps. All time-resolved data were analyzed using the Glotaran package for global analysis[35]. Results of the analysis are plotted in terms of a species associated spectra assuming a sequential reaction scheme.

Acknowledgement

We acknowledge Dr. Pavel Müller (CEA Saclay) for providing digital forms of the FAD model spectra.

Keywords: Amino acids • Biophysics • Radicals • Time-resolved spectroscopy • UV/Vis spectroscopy

[1] K. S. Conrad, C. C. Manahan, B. R. Crane, *Nature Chem. Biol.* **2014**, *10*, 801

[2] A. Gräslund, M. Sahlin, B.-M. Sjöberg, *Env. Health Persp.* **1985**, *64*, 139-149

[3] P. Müller, J.-P. Bouly, K. Hitomi, V. Balland, E. D. Getzoff, T. Ritz, K. Brettel, *Sci. Rep.* **2014**, *4*, 5175

[4] C. Aubert, M. H. Vos, P. Mathis, A. P. M. Eker, K. Brettel, *Nature* **2000**, *405*, 586-590

[5] J. Brazard, A. Usman, F. Lacombat, C. Ley, M. M. Martin, P. Plaza, L. Mony, M. Heijde, G. Zabulon, C. Bowler, *J. Am. Chem. Soc.* **2010**, *132*, 4935-4945

[6] Z. Liu, C. Tan, X. Guo, J. Li, L. Wang, A. Sancar, D. Zhong, *Proc. Natl. Acad. Sci. U.S.A.* **2013**, *110*, 12966-12971

[7] A. Lukacs, A. P. M. Eker, M. Byrdin, K. Brettel, M. H. Vos, *J. Am. Chem. Soc.* **2008**, *130*, 14394-14395

[8] K. Maeda, A. J. Robinson, K. B. Henbest, H. J. Hogben, T. Biskup, M. Ahmad, E. Schleicher, S. Weber, C. R. Timmel, P. J. Hore, *Proc. Natl. Acad. Sci. U.S.A.* **2012**, *109*, 4774

[9] Y. Fukushima, K. Okajima, Y. Shibata, M. Ikeuchi, S. Itoh, *Biochemistry* **2005**, *44*, 5149-5158

[10] M. Gauden, J. S. Grinstead, W. Laan, I. H. M. van Stokkum, M. Avila-Perez, K. C. Toh, R. Boelens, R. Kaptein, R. van Grondelle, K. J. Hellingwerf, J. T. M. Kennis, *Biochemistry* **2007**, *46*, 7405-7415

[11] A. Lukacs, R. Brust, A. Haigney, S. P. Laptenok, K. Addison, A. Gil, M. Towrie, G. M. Greetham, P. J. Tonge, S. R. Meech, *J. Am. Chem. Soc.* **2014**, *136*, 4605-4615

[12] S. P. Laptenok, L. Bouzhir-Sima, J.-C. Lambry, H. Myllykallio, U. Liebl, M. H. Vos, *Proc. Natl. Acad. Sci. U.S.A.* **2013**, *110*, 8924-8929

[13] H. Yang, G. Luo, P. Karnchanaphanurach, T.-M. Louie, I. Rech, S. Cova, L. Xun, X. S. Xie, *Science* **2003**, *302*, 262-266

[14] L. Nag, P. Sournia, H. Myllykallio, U. Liebl, M. H. Vos, *J. Am. Chem. Soc.* **2017**, *139*, 11500-11505

[15] M. Gauden, I. H. M. van Stokkum, J. M. Key, D. C. Lührs, R. van Grondelle, P. Hegemann, J. T. M. Kennis, *Proc. Natl. Acad. Sci. U.S.A.* **2006**, *103*, 10895-10900

[16] G. Renger in *Natural and Artificial Photosynthesis,* (Ed. R. Razeghifard), John Wiley & Sons, Ltd, **2013**, pp. 65-119

[17] A. Crueger, W. Crueger in *Microbial Enzymes and Biotechnology,* (Eds.: W. M. Fogarty, C. T. Kelly), Springer Netherlands, Dordrecht, **1990**, pp. 177–226

[18] I. A. Rasiah, K. H. Sutton, F. L. Low, H.-M. Lin, J. A. Gerrard, *Food Chem.* **2005**, *89*, 325 - 332

[19] J. Afseth, G. Rølla, *Caries Res.* **1983**, *17*, 472-475

[20] T. Chen, S. C. Barton, G. Binyamin, Z. Gao, Y. Zhang, H.-H. Kim, A. Heller, *J. Am. Chem. Soc.* **2001**, *123*, 8630-8631

[21] S. B. Bankar, M. V. Bule, R. S. Singhal, L. Ananthanarayan, *Biotechnol. Adv.* **2009**, *27*, 489 - 501

[22] G. Wohlfahrt, S. Witt, J. Hendle, D. Schomburg, H. M. Kalisz, H.-J. Hecht, *Acta Crystal. Sect. D* **1999**, *55*, 969–977

[23] N. Mataga, H. Chosrowjan, Y. Shibata, F. Tanaka, *J. Phys. Chem. B* **1998**, *102*, 7081-7084

[24] N. Mataga, H. Chosrowjan, Y. Shibata, F. Tanaka, Y. Nishina, K. Shiga, *J. Phys. Chem. B* **2000**, *104*, 10667-10677

[25] D. Zhong, A. H. Zewail, *Proc. Natl. Acad. Sci. U.S.A.* **2001**, *98*, 11867-11872

[26] A. Fujiwara, Y. Mizutani, *J. Raman Spectrosc.* **2008**, *39*, 1600-1605

[27] A. Lukacs, R.-K. Zhao, A. Haigney, R. Brust, G. M. Greetham, M. Towrie, P. J. Tonge, S. R. Meech, *J. Phys. Chem. B* **2012**, *116*, 5810-5818

[28] V. Massey, R. G. Matthews, G. P. Foust, L. G. Howell, C. H. Williams, G. Zanetti, S. Ronchi in *Pyridine Nucleotide-Dependent Dehydrogenases: Proceedings of an Advanced Study Institute held at the University of Konstanz, Germany,* (Ed. H. Sund), Springer Berlin Heidelberg, Berlin, Heidelberg, **1970**, pp. 393-411

[29] J. Pan, M. Byrdin, C. Aubert, A. P. M. Eker, K. Brettel, M. H. Vos, *J. Phys. Chem. B* **2004**, *108*, 10160-10167

[30] S. Solar, N. Getoff, P. S. Surdhar, D. A. Armstrong, A. Singh, *J. Phys. Chem.* **1991**, *95*, 3639-3643

[31] K. Brettel, M. Byrdin, M. H. Vos in *Ultrafast Dynamics at the Nanoscale: Biomolecules and Supramolecular Assemblies,* (Eds.: S. Haacke, I. Burghardt), Pan Stanford, Singapore, **2016**, pp. 65-90

[32] C. Aubert, P. Mathis, A. P. M. Eker, K. Brettel, *Proc. Natl. Acad. Sci. U.S.A.* **1999**, *96*, 5423-5427

[33] M. Kundu, T.-F. He, Y. Lu, L. Wang, D. Zhong, *J. Phys. Chem. Lett.* **2018**, *9*, 2782-2790

[34] S. P. Laptenok, P. Nuernberger, A. Lukacs, M. H. Vos in *Methods in Molecular Biology, Fluorescence Spectroscopy and Microscopy: Methods and Protocols, Vol. 1076,* (Eds.: Y. Engelborghs, A. J. W. G. Visser), Humana Press, New York, **2014**, pp. 321-336

[35] J. J. Snellenburg, S. P. Laptenok, R. Seger, K. M. Mullen, I. H. M. van Stokkum, *J. Stat. Software* **2012**, *49*

Entry for the Table of Contents

COMMUNICATION

Full spectral characterisation of flavin excitation-photoproducts on the few picosecond timescale in the model flavoprotein glucose oxidase reveals the implication of tyrosine cation radicals, suggesting a potential role of this species as intermediate in biochemical electron transfer reactions.

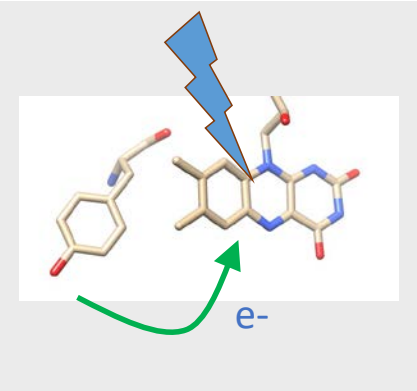

*Lipsa Nag, Andras Lukacs, Marten H. Vos**

Page No. – Page No.

Short-lived radical intermediates in the photochemistry of glucose oxidase